

## SCIENCE OF TSUNAMI HAZARDS

Journal of Tsunami Society International

Volume 38

Number 2

2019

### THE BEHAVIOR OF A TSUNAMI-LIKE WAVE PRODUCED BY DAM BREAK AND ITS RUN-UP ON 1:20 SLOPE

Benazir<sup>1</sup>, Radianta Triatmadja<sup>2\*</sup>, Adam Pamudji Rahardjo<sup>2</sup>, and Nur Yuwono<sup>2</sup>

<sup>1</sup>Doctoral Student at Dept of Civil and Environmental Engineering, Faculty of Engineering Universitas Gadjah Mada, Indonesia.

<sup>2</sup>Department of Civil and Environmental Engineering, Faculty of Engineering Universitas Gadjah Mada, Indonesia.

\*Corresponding author: [radiana@ugm.ac.id](mailto:radiana@ugm.ac.id), Kompleks Yadara V/12 Babarsari Yogyakarta, Indonesia, 55281.

#### ABSTRACT

A solitary wave is commonly used in tsunami study for both physical and numerical models. A tsunami is categorized as a long wave which drastically changes its shape and speed when propagates in shallow water and land. In this paper, a physical model test of tsunami propagation based on Dam Break system to produce a tsunami-like wave was carried out. In a flume, finite reservoir length is set to sufficiently provide downstream length for propagation and run-up area. The downstream part is divided into two sections of bed configuration where it has flatbed as shallow water region and 1:20 of sloping beach model. The effect of the ratio of the reservoir depth to the initial downstream depth ( $d_0/d_1$ ) is discussed. In addition, the tsunami inundation depth and run-up in land were also investigated. For comparison of results, numerical model similar to the physical one was conducted. The numerical model was based on a set of nonlinear shallow water equation that employed second-order explicit leap-frog finite difference scheme. The use of numerical approach using shallow water equation may not yield realistic results since the wave evolution in shallow water and coastal area has not sufficiently accommodated. The comparison between the models suggested that the numerical model consistently produce slightly higher run-up than its counterpart. This was probably due to the application of shallow water equation (SWE) in the numerical model which could not entirely solve vertical convection problems, breaking waves, and turbulence-related aspects that reduced run-ups energy. A fine

*Vol. 38, No. 2, page 49 (2019)*

tuning method to improve the numerical model run-ups is necessary by introducing proper artificial energy reduction mechanism in the numerical model especially at breaking condition.

**Keywords:** *bore; modeling; long wave; dam break; inundation.*

## 1. INTRODUCTION

Tsunami that is triggered by tectonic activity, especially earthquake on the ocean floor is relatively small in amplitude at fault location or in deep sea. Its velocity decreases dramatically when the wave reaches the shallow water with decreasing water depth. In this phase, the wave height is increased and suddenly transformed to breaking wave. Since tsunami is a long wave it makes the flow effortlessly towards the mainland and cause damage and flooding. Tsunami surge that propagates in shallow water and coastal plain is in some criteria like the wave that was produced by the failure of a reservoir or dam break (Chanson, 2006). Based on some documentation in tsunami event, the wave characteristics tend to break as bore when traveling to the coastline (nearshore) i.e. the wave propagation in Kuji Bay during Tsunami Tohoku 2011. Previously, Shuto (1997) observed Tsunami at Showa 1933 which indicated that for tsunami with a wave height of more than 4 m, a plunging breaking type occurs in shallow water.

The first study of single long wave study approaching a coastal slope was, among others, performed by Hall & Watt (1953). This physical experiment realized the 1+1 one-dimensional long wave theory, which generated long wave over a constant depth, evolving to a constant depth, and then climbing a sloping beach. Miller (1968) also conducted laboratory work by tested wave propagation on four slope variations. The development of tsunami hydrodynamics began in the early 1980s that focused solitary waves as the initial condition (Synolakis & Bernard, 2006). In the late 1980s, Synolakis (1986) and Synolakis (1987) accomplished the Initial Value Problem (IVP) of the Nonlinear Shallow Water Equation (NLSWE) for solitary wave propagation over a constant water depth until run-up to the sloping beach. Synolakis (1987) derived the equation which is then known as "Run-up Law" for solitary wave propagation on the sloping beach and compared it with relevant laboratory results. The discussion about tsunami waveform during its propagation over constant depth was also done by Yeh and Ghazali (1986). It seemed that breaking and non-breaking condition depended on the initial condition of a simulation setup. This research aims to discuss tsunami-like waveforms over constant depth and sloping beach that was initiated by Dam Break method.

## 1. LITERATURE REVIEW

Tsunami run-up formulae have been developed using various approaches. Early in its development, the run-up relationships were associated with wavelength and wave height at the shore as done by Kaplan (1955); Shuto (1967); and Togashi (1981). Freeman and Le Mehaute (1964) predicted run-up that was affected by the horizontal velocity component when it reached the shoreline without considering beach slope variable. The derivation of an analytical equation from the laboratory work by using shallow water wave theory was also done by Synolakis (1986) and (1987). Li & Raichlen (2003) and Zhao et al. (2012) also conducted a study of the tsunami

run-up model in which the energy variables changed when the wave reached the coastal land. The common run-up formulae used today are shown in Table 1.

Long wave amplitude increases as it travels in sloping shallow water until the wave eventually breaks. Bore height is usually the main parameter associated with the run-up process. Baldock & Holmes (1999) analytically derived the formula (Table 1) based on run-up and run-down (swash) oscillation with a bore waveform. In obtaining the equation, they also studied the energy transfer around the coastline. The equation describes that the unsaturated run-up (i.e. the same run-up as the first swash) as a function of flow velocity or bore height ( $H_B$ ). The coefficient of  $C_k$  is kinetic energy converted into potential energy during run-up which equals 2. Then, it indicates that the run-up height is twice the bore height ( $R = 2H_B$ ). This coefficient is the same as in Yeh et al. (1989) which is called bore collapse.

Table 1. The existing non-dimensional tsunami run-up equations.

Waveform	Non-Dimensional Run-up ( $R/d_1$ )	Equation No.	Reference
Solitary	$11(\beta)^{0.67}(H/d_1)^{1.9(\beta)^{0.35}}, \beta = 5^\circ - 12^\circ$ $3.05(\beta)^{-0.13}(H/d_1)^{1.15(\beta)^{0.02}}, \beta = 12^\circ - 45^\circ$	(1)	Hall & Watt (1953)
Solitary	$2.831\sqrt{\cot\beta}\left(\frac{H}{d_1}\right)^{1.25}$	(2)	Synolakis (1987)
Solitary	$1.109\left(\frac{H}{d}\right)^{0.582} \text{ (max)}$ $0.918\left(\frac{H}{d}\right)^{0.606} \text{ (avg)}$	(3a) (3b)	Synolakis (1987)
N-wave	$3.3\varepsilon_g p_0^{\frac{1}{4}} Q(L, \gamma_s) \frac{R_{sol}}{d_1}$	(4)	Tadepalli & Synolakis (1996)
Bore	$\frac{U_0^2}{2gd_1} = \frac{C_k^2 H_B}{2d_1}$	(5)	Baldock & Holmes (1999)
Bore	$\frac{U^{*2}}{2gd_1}$	(6)	Shen & Meyer (1963)
N-Wave	$3.86\sqrt{\cot\beta}\left(\frac{H}{d_1}\right)^{1.25}$	(7)	Tadepalli & Synolakis (1994)
Double N-Wave	$4.55\sqrt{\cot\beta}\left(\frac{H}{d_1}\right)^{1.25}$	(8)	Tadepalli & Synolakis (1994)

## 2. RESEARCH METHOD

A physical simulation of tsunami propagation and run-up using Dam Break method was implemented in a laboratory flume. This simulation focused on wave propagation in constant depth or shallow water region, wave propagation on shore, run-up and inundation. The mechanism of tsunami generation and propagation using Dam Break method and its variables are shown in Figure 1. This physical work was performed in a channel of 15.00 m long by 0.60 m wide and 0.44 m in height. The downstream depth ( $h$ ) represented the constant depth of the sea water near the coast. As can be seen in the figure that the channel was divided into two regions, i.e. the upstream region of 4 m as a reservoir and downstream region of 11 m as a coastal model profile which was separated by a sluice gate. Along the downstream region, there was 3 m long horizontal bottom profile (constant depth zone) as shallow water area followed by a beach model (sloping zone) with a uniform slope of 1:20 which may be categorized as a mild slope. Thus, the source of tsunami generation (gate) was 4 m for  $h = 0.05$  m and 5 m for  $h = 0.10$  m from the coastline. The experiment was set up to obtain typical bore formations and to get more complete data to examine the bore characteristics resulting from a Dam Break method, especially, when the bore propagated on a constant depth before run-up on land. This method has been commonly used to model tsunami that arrived in shallow water region and on land such as by Chanson (2005); Triatmadja & Nurhasanah (2012); and Triatmadja & Benazir (2014).

Using Dam Break method, waves were formed by the rapid released of the gate (using quickly released mechanism). The gate opening depended on the load that was connected to the gate. The load weight can be calculated based on Triatmadja (2010) for high opening speeds so that the gate can be considered instantaneously (ranging from 0.1-0.4 seconds depending on the reservoir depth). The wave behavior, including the height and velocity, downstream of the channel was affected by the reservoir depth as well as the downstream depth. The difference between the reservoir and the downstream depth defined the generated wave height while the ratio of reservoir depth to the downstream depth affect more specifically on the bore behavior. Based on Yeh et al. (1989), the behavior of bore formation was presented at the initial simulation for parameter  $\beta$ , which was classified as fully developed bore and undular bore. In this study, two variations for  $\beta$  were applied, i.e. 0.05 m and 0.10 m which were tested with four reservoir depths, i.e. 0.30 m, 0.25 m, 0.20 m, and 0.15 m. A mini pump was used to make sure that the depth in both regions has sufficiently accurate as shown in Figure 2 (right).

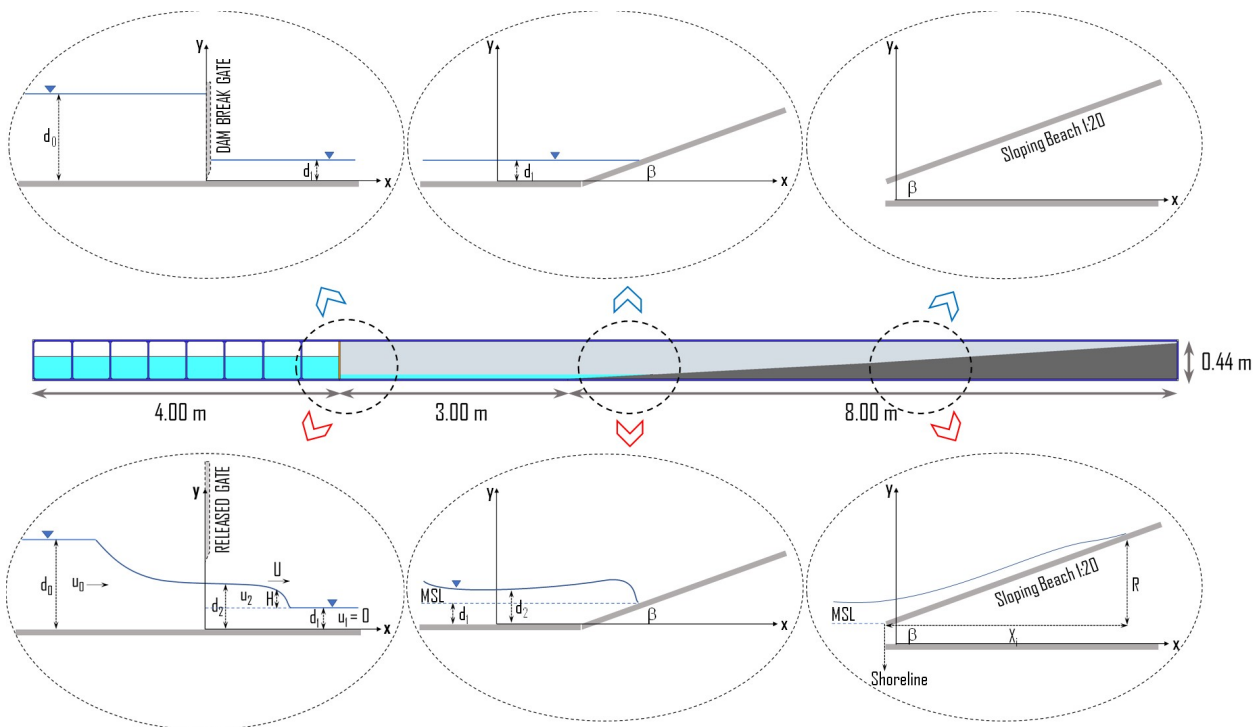


Figure 1. The mechanism of wave generation using Dam Break method and its variables

Wave probes were used to retrieve the water fluctuation over time. There were four sensors used in this test, which were placed at 2, 3, 4, and 5 m from the dam gate as portrayed in Figure 2 (left). The sensors were calibrated before they were used for data acquisition.

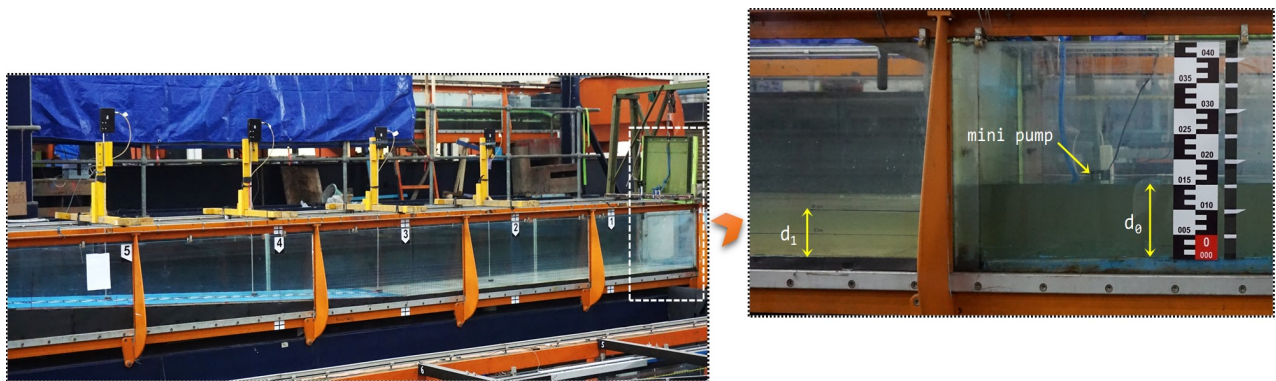


Figure 2. The downstream and upstream of wave flume

To study the wave behavior that traveled along the channel, five cameras (Cam) were placed in the simulation area. Cam-1 was placed near the dam gate to record the waveform when the gate was opened. Cam-2 was positioned in the upstream of the channel to record the wave propagation, especially when it began to climb the coastal slope. Cam-3 was used to observe details of wave propagation over the constant depth and when it began climbing on the coastal slope. This camera

was capable of recording video up to 60 fps (frame per second) with Full High Definition (FHD) quality. For recording the entire simulation area, Cam-4 was placed farther away from Cam-3. Finally, for close examination of the inundation height and length, the simulation was equipped with Cam-5.

Numerical simulation was performed and was verified using the physical model. The same cases were simulated using the main program of Goto et al. (1997) and Imamura et al. (2006). The program was slightly modified where some additional input-output facilities were added for convenience and rewrote the program in Visual Basic .Net programming language. The program uses second-order explicit leap-frog finite difference scheme to discretize a set of Nonlinear Shallow Water Equation (NSWE). For the propagation of tsunami in the shallow water, the horizontal eddy turbulence terms are negligible as compared with the bottom friction. The equations are written in Cartesian coordinate as (Imamura et al., 2006):

$$\frac{\partial \eta}{\partial t} + \frac{\partial M}{\partial x} + \frac{\partial N}{\partial y} = 0 \quad (9a)$$

$$\frac{\partial M}{\partial t} + \frac{\partial}{\partial x} \left( \frac{M^2}{D} \right) + \frac{\partial}{\partial y} \left( \frac{MN}{D} \right) + gD \frac{\partial \eta}{\partial x} + \frac{\tau_x}{\rho} = 0 \quad (9b)$$

$$\frac{\partial M}{\partial t} + \frac{\partial}{\partial x} \left( \frac{MN}{D} \right) + \frac{\partial}{\partial y} \left( \frac{N^2}{D} \right) + gD \frac{\partial \eta}{\partial y} + \frac{\tau_y}{\rho} = 0 \quad (9c)$$

$D = h + \eta$  is the total water depth where  $h$  is the still water depth and  $\eta$  is the sea surface elevation.  $M$  and  $N$  are the water velocity fluxes in the  $x$  and  $y$  directions, respectively

$$M = \int_h^\eta u dz = u(h + \eta) = uD \quad (10a)$$

$$N = \int_h^\eta v dz = v(h + \eta) = vD \quad (10b)$$

Bottom friction in the  $x$  and  $y$  direction are respectively represented by terms  $\tau_x$  and  $\tau_y$ , which is a function of friction coefficient  $f$ . This coefficient can be computed from Manning roughness ( $n_0$ ) by the following relationship

$$n_0 = \sqrt{\frac{fD^{1/3}}{2g}} \rightarrow f = \frac{n_0^2 2g}{D^{1/3}} \quad (11)$$

Eq. (11) describes that the friction coefficient increases when the total water depth decreases. Manning roughness is usually chosen as a constant for a given condition of sea bottom, then the bottom friction terms are expressed by

$$\frac{\tau_x}{\rho} = \frac{1}{2} \frac{f}{D^2} M \sqrt{M^2 + N^2} \quad (12a)$$

$$\frac{\tau_y}{\rho} = \frac{1}{2} \frac{f}{D^2} N \sqrt{M^2 + N^2} \quad (12b)$$

In this research, Manning coefficient ( $n$ ) of 0.012 was used to describe the bed slope that was made of plywood. Other numerical parameters are listed in Table 2.

Table 2. Parameters that were used in the numerical model

Grid Numbers		Grid Size (m)		DT	Total Time
x	y	x	y	(s)	(s)
1500	60	0.01	0.01	0.0025	180

### 3. RESULT AND DISCUSSION

#### 1. Tsunami Generation on Laboratory Scale using Dam Break Method

The tsunami flowed easily towards mainland due to its long wave characteristics and normally caused flooding. Based on some criteria, tsunami surge that propagates in shallow water and coastal plain is similar to the wave that was produced by the failure of reservoir or dam break (Chanson, 2006). Figure 3 shows a wave propagation stage from a laboratory test where  $h = 2.0$  and  $h_0 = 0.10$  m. The front velocity was relatively high when it traveled at the constant depth depending on  $h$ . Figure 3 (top left) shows the wave front location at  $x = 2$  m at  $t = 1.07$  s after which the wave propagated at the sloping zone and reached the coastline, i.e. at  $x = 5$  m at  $t = 3.07$  s. The waves propagated faster for the same  $h$  when  $h > 2.0$ . On land, the front velocity decreased and continued to climb the beach slope profile to the maximum run-up at  $x = 7.63$  m followed by the run-down phase.

The wave height fluctuated during the travel time for each model of beach profile. As mentioned earlier the wave height was defined by the difference between the  $h$  and  $h_0$ . The larger  $h$  was the value of  $h$  and  $h_0$  yielded the higher wave heights in the downstream. In addition, the recorded wave fluctuations also vary over the measurement locations. In shallow water, the recorded wave was relatively smaller than on land. The change in wave height was caused by changes in water depth or shoaling process. It followed by a condition where the wave crest became unstable which subsequently turns into breaking waves. It should be noted that when the wave height reached the maximum conditions on the ground, the front velocity decreased drastically as also observed by Lukkunaprasit et al. (2009). The vertical release of the gate on Dam Break method caused the flow below the gate to advance first which cause water to jump downstream of it. For a region close to the gate and in a very short time, such impulse affects the wave generation. For more details, the water fluctuations along the channel with two downstream depth variations are shown in Figure 4. Based on the measurement along the channel, it was found that the waves were higher on land rather than in the water.

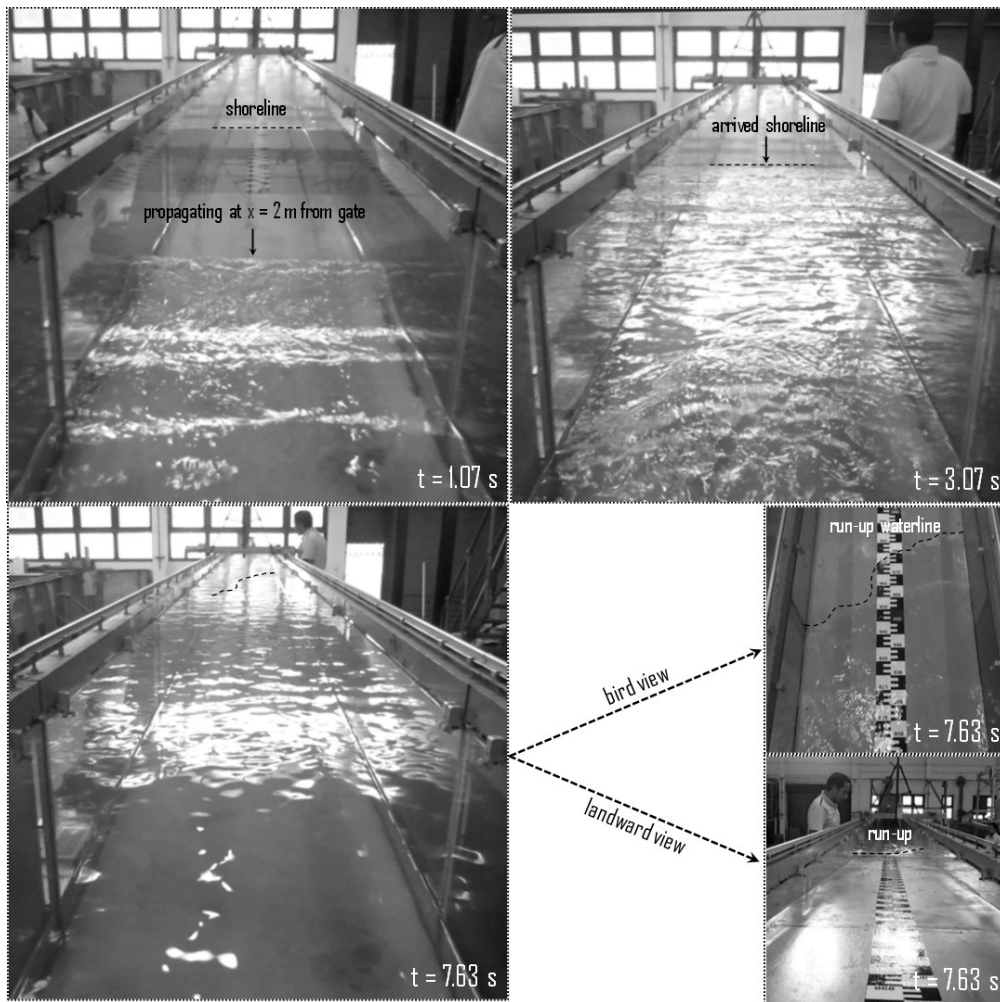


Figure 3. Surge resulted from Dam Break method in wave flume for  $\beta = 2.0$  and  $\gamma = 0.10$  m

The wave height fluctuated during the travel time for each model of beach profile. As mentioned earlier the wave height was defined by the difference between the  $\beta$  and  $\gamma$ . The larger was the value of  $\beta$  and  $\gamma$  yielded the higher wave heights in the downstream. In addition, the recorded wave fluctuations also vary over the measurement locations. In shallow water, the recorded wave was relatively smaller than on land. The change in wave height was caused by changes in water depth or shoaling process. It followed by a condition where the wave crest became unstable which subsequently turns into breaking waves. It should be noted that when the wave height reached the maximum conditions on the ground, the front velocity decreased drastically as also observed by Lukkunaprasit et al. (2009). The vertical release of the gate on Dam Break method caused the flow below the gate to advance first which cause water to jump downstream of it. For a region close to the gate and in a very short time, such impulse affects the wave generation. For more details, the water fluctuations along the channel with two downstream depth variations are shown in Figure 4. Based on the measurement along the channel, it was found that the waves were higher on land rather than in the water.



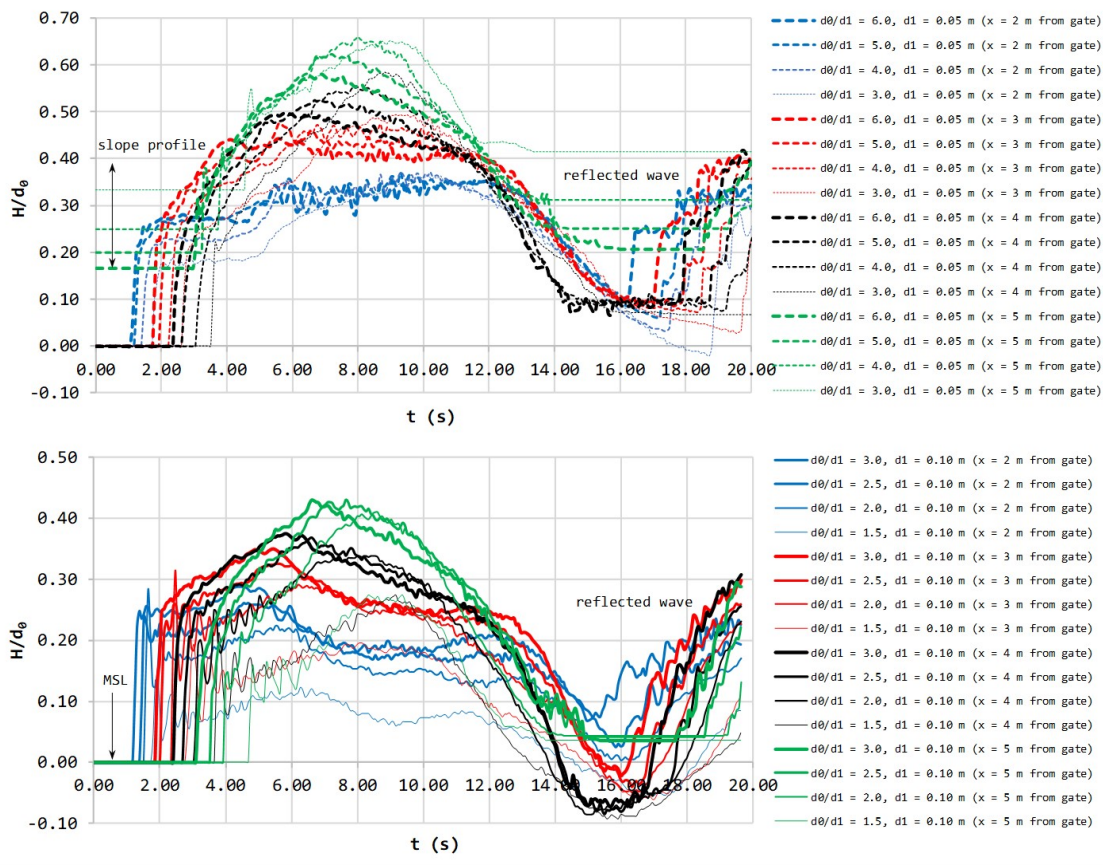


Figure 4. Water fluctuation along the channel by physical model tests for  $d_1 = 0.05$  m (above) and  $0.10$  m (below).

The simulation of tsunami model by Dam Break approach requires an adequately long channel to accommodate run-up and run-down processes. However, if the study concern only to the surge front force parameters during run-up as done by Triatmadja & Nurhasanah (2012) and Triatmadja & Benazir (2014), longer channel may not be necessary. In this study, run-up and run-down processes were observed, where the reflected waves from the upstream end of the channel should not be allowed to affect the result. To satisfy this condition, the reservoir depth used was  $0.30$  m,  $0.25$  m,  $0.20$  m, and  $0.15$  m whilst the reservoir length was adjusted to minimize the effect of upstream wall reflection on run-up and run-down. In the previous research schemes (Benazir et al. 2016a and 2016b), the reservoir length was  $7.90$  m which was reduced to  $4.00$  m in the present research. With these adjustments, the reflection occurred at the time when the run-down process ends. This allowed for an additional mechanism to totally remove the reflection (due to the upstream wall of the channel) by adding one more gate at downstream of the main gate as done by Kuswandi et al. (2017).

## 1. Wave Propagation in Constant Depth and Sloping Zone

Observations on the physical model of wave propagation in constant water were carried out. Four types of initial waveform were simulated at two different downstream depths ( $d_1 = 0.05$  m and  $d_1 = 0.10$  m) so that there were 8 (eight) waveforms with different height and behavior. The observation was repeated three times for each scenario and the results are shown in Figure 5. The parameter  $d_0/d_1$  was used to discuss the waveforms.

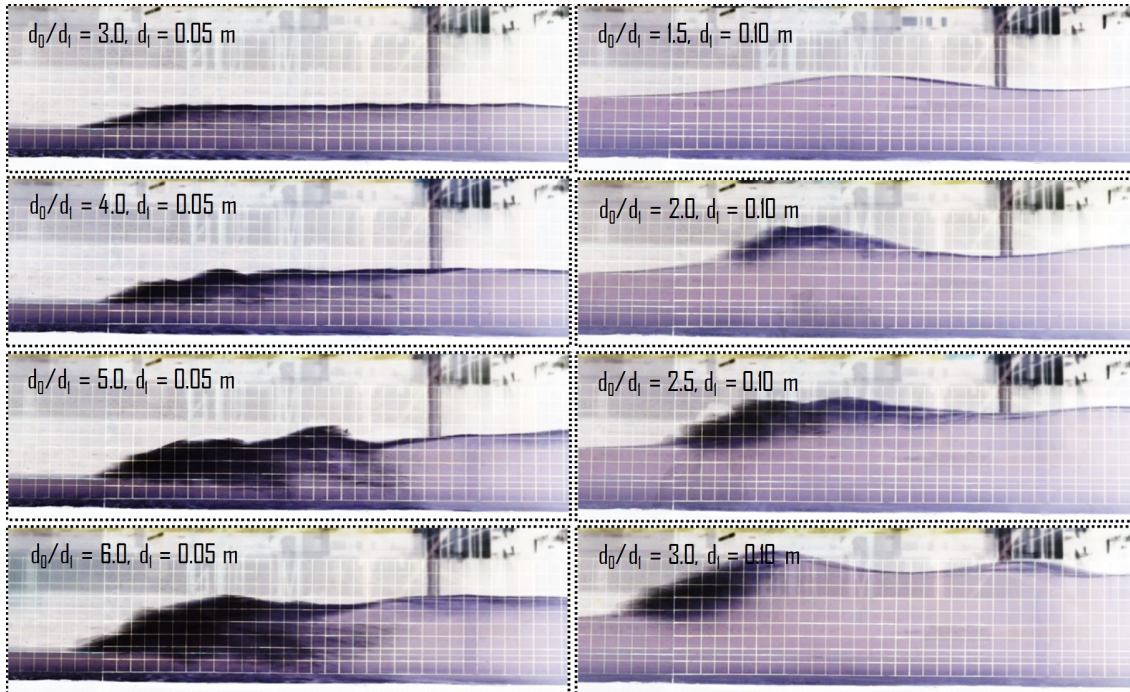


Figure 5. Bore variations in constant depth at  $x = 2$  m for all scenarios of the tested model (grid size is 0.02 m)

Based on visual observation, at  $x = 2$  m from the source, the waveforms were almost entirely bore, except for  $d_0/d_1 = 1.5$  (Fig. 5). This indicates that the developed bore was formed with the  $d_0/d_1 \geq 2.0$ . When  $d_0/d_1 < 2.0$  such as for  $d_0/d_1 = 1.5$  as shown in Figure 5, undular bore type was produced. This is due to the linear effect of significant frequency dispersion (Yeh & Ghazali, 1986). The undular bore transformation occurred when it traveled in the reducing depth (Fig. 6).

Figure 5 shows the shape of the wave fronts that was fully broken with high turbulence for all  $d_0/d_1 = 6.0, d_0/d_1 = 5.0, d_0/d_1 = 4.0,$  and  $d_0/d_1 = 3.0$ . The difference was apparent from the scale of the bore strength, such as for  $d_0/d_1 = 6.0$  and  $d_0/d_1 = 5.0$ . According to Yeh et al. (1989), the scale of bore strength in the natural coast is limited by the mechanism of wave breaking. With the downstream depth of  $d_1 = 0.10$  m, the strength ranged from  $d_0/d_1 = 1.5$  to  $d_0/d_1 = 3.0$  where the bore formation was partially developed (except for  $d_0/d_1 = 1.5$ ). This partly developed bore was strongly turbulent (breaking wave) at the front of the bore whilst in the rear side such formation was not noticeable. However, the partly developed bore

formation was later transformed into fully developed bore during its travel as the depth reduced, as shown in Figure 7 for  $d_0/d_1 = 2.0$ . For  $d_0/d_1 > 2.0$ , the transformation to fully developed bore was indicated by its form which was more transient with higher turbulence.

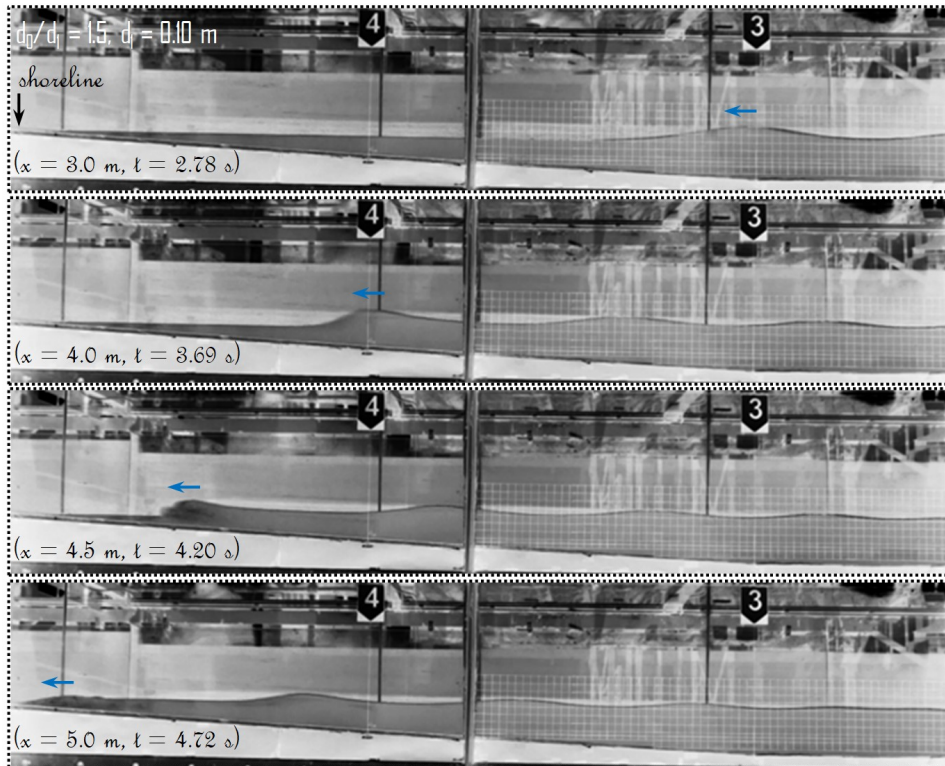


Figure 6. Wave propagation and transformation in sloping zone for  $d_0/d_1 = 1.5$  and  $d_1 = 0.10$  m

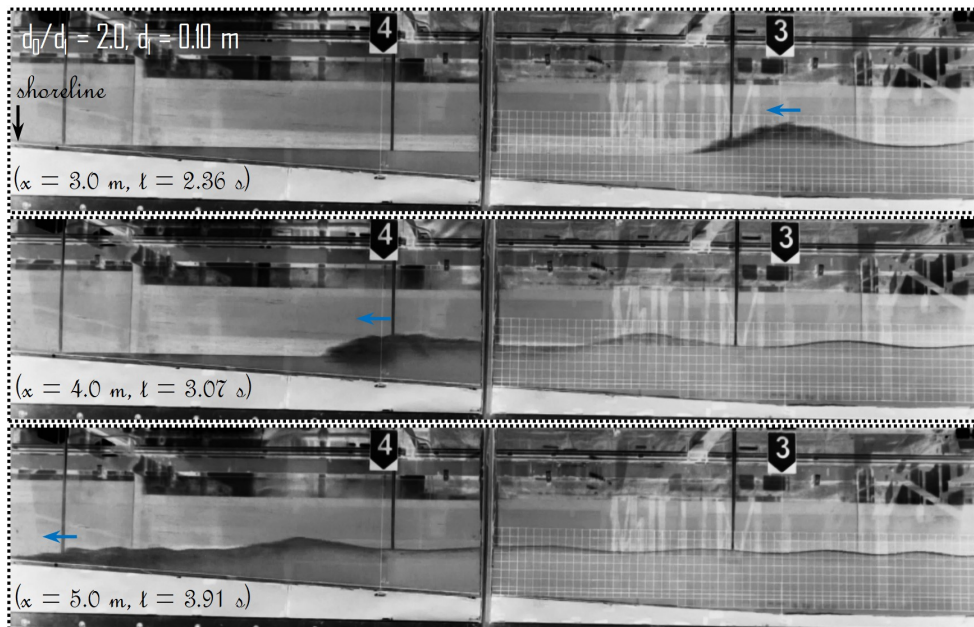


Figure 7. Formation of fully developed bore for  $d_0/d_1 = 2.0$  in the sloping zone



In Yeh & Ghazali (1986), Yeh et al. (1989), and Yeh (1991), the space for bore to develop after its generation (the length of constant bottom profile) was limited to 0.4 m. In this research, the length of this profile was 3 m or totally 4 m for  $d_0 = 0.05$  m and 5 m for  $d_0 = 0.10$  m including the additional sloping zone. Therefore, the undular form and partly developed bore may develop into fully developed bore when the wave travels to the beach. The total depths fluctuations at the constant depth zone depending on  $d_0$  and  $d_1$  are given in Figure 8.

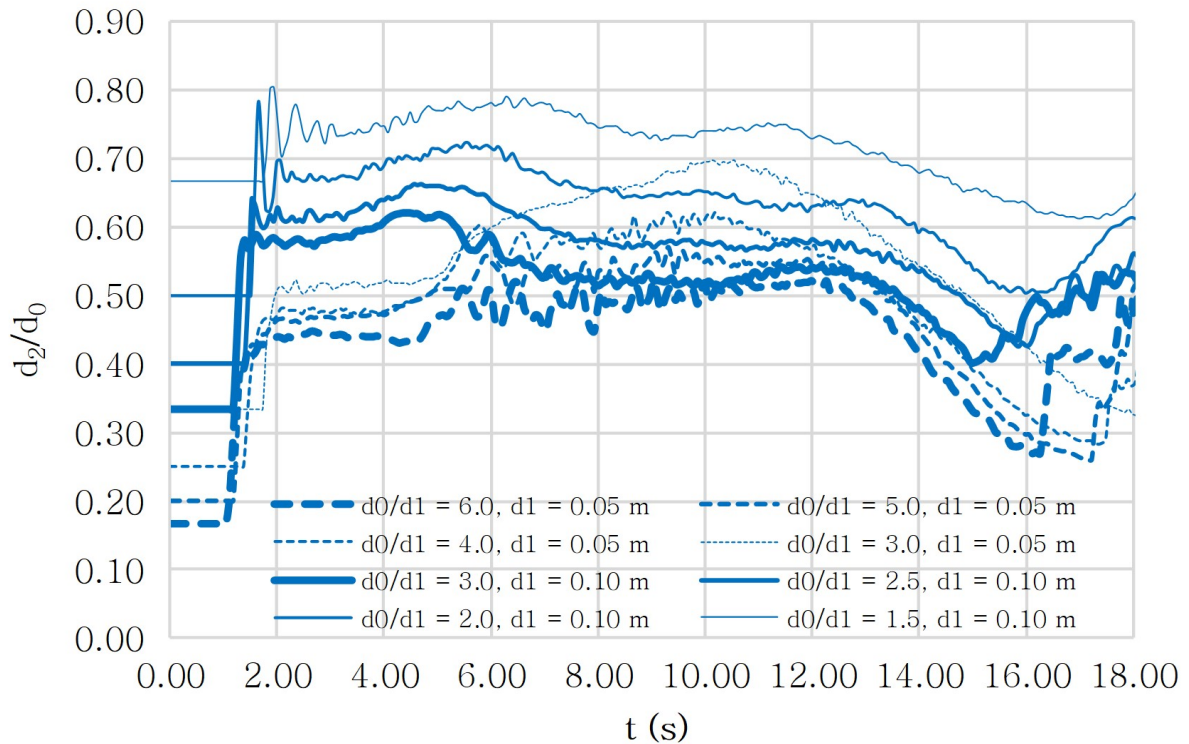


Figure 8. Fluctuations of total depth over time at constant depth zone for  $d_1 = 0.05$  m (dash line) and  $d_1 = 0.10$  m (solid line)

The front velocity in constant depth zone was given as a function of total depth of water ( $d_2$ ) in Figure 9. The front velocity at  $d_1 = 0.10$  m was greater than  $d_1 = 0.05$  m and the measured velocity was plotted in Figure 9 against  $d_2$ . The analytical solutions from Chanson (2005) or (2006) predicted a very similar velocity for both  $d_1 = 0.10$  m and  $d_1 = 0.05$ . The analytical line calculated based on Chanson's solutions has been extended to  $d_0 = d_2 = d_1$  when theoretically the velocity of the surge front is  $U = \sqrt{gd_2}$ . This is the minimum theoretical velocity of the surge front in this experimental case. Other experimental data of Dam break surge velocities from Arnason et al. (2009) are also plotted in Figure 9. Arnason et al. (2009) experiment agreed with analytical solutions (calculated by the authors based on Arnason's data). They used  $d_1 = 0.02$  m whilst  $d_0$  varied from 0.10 to 0.30 m.

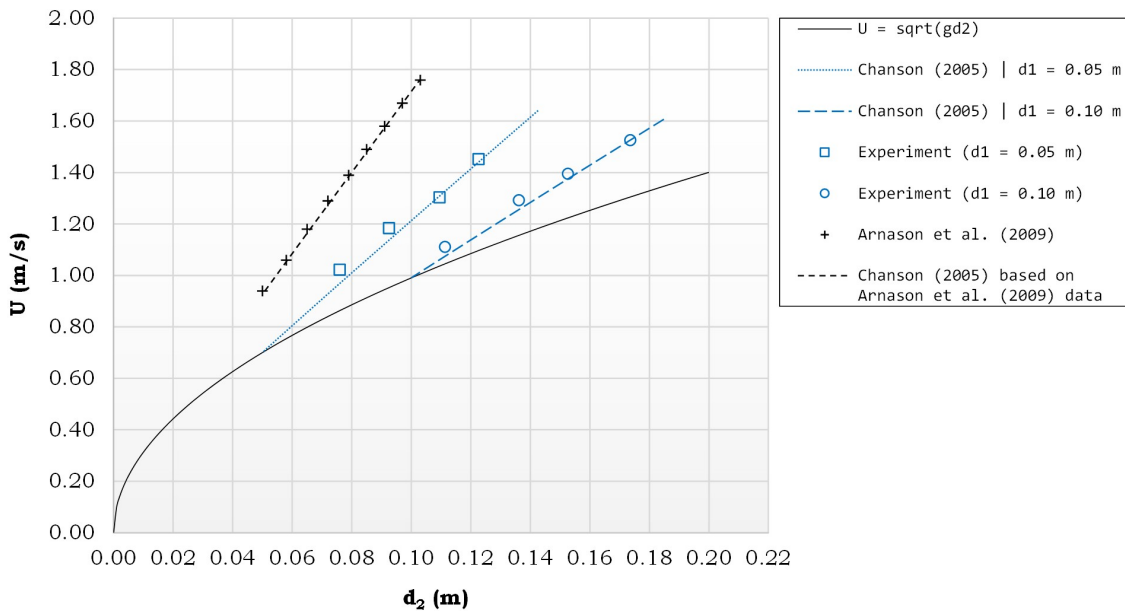


Figure 9. The relationship of front velocity and total depth of wave at a constant depth

### 1. Tsunami Run-up on Uniformly Sloping Beach 1:20

The surge velocity decreases as the influence of roughness and the effect of beach slope become more dominant. Figure 10 shows the surge velocity in the coastal area of the present model, which was calculated based on surge propagation in between  $x = 4$  m and  $x = 6$  m for  $d_1 = 0.05$  m and in between  $x = 5$  m and  $x = 7$  m for  $d_1 = 0.10$  m on dry land. It is seen that the wave Froude number for  $d_1 = 0.05$  m was less than for  $d_1 = 0.10$  m for the same  $d_2$ . For the same the Froude number of the surge was greater at higher  $d_2$ . The difference is more pronounced at lower  $d_2$ . One of the reason is due to more turbulence and hence more energy dissipation at smaller  $d_2$  or shallower water. In this case,  $d_2$  was the inundation depth at the coastline.

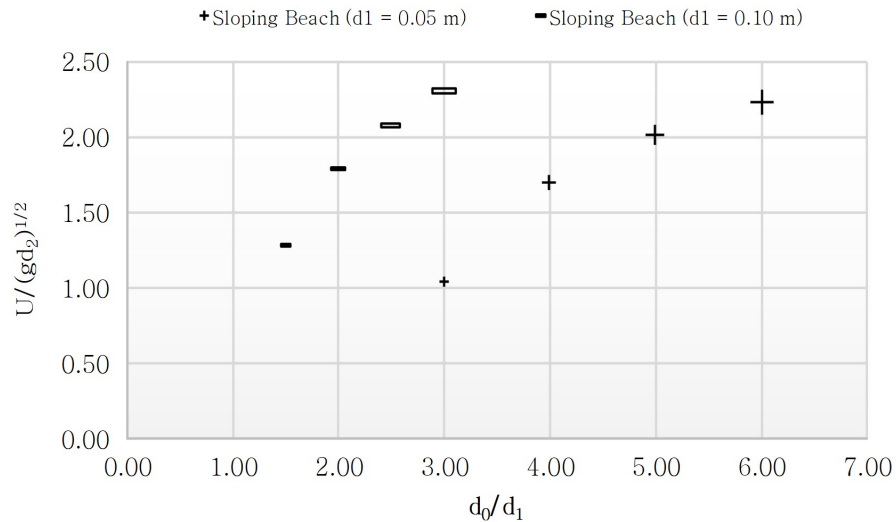


Figure 10. Front velocity in the coastal area

To compare between the physical, the numerical model results and with some analytical solutions, a non-dimensional relationship namely  $H/d_1$  and  $R/d_1$  parameters were used. The experimental data and analytical solutions of run-up are plotted in Figure 11. The variable  $H$  is the wave height ( $d_2 - d_1$ ) in shallow water, i.e. at  $x = 2$  m in the present physical and numerical experiment and the solitary wave height in all other experiments. The run-up is represented by  $R$ .

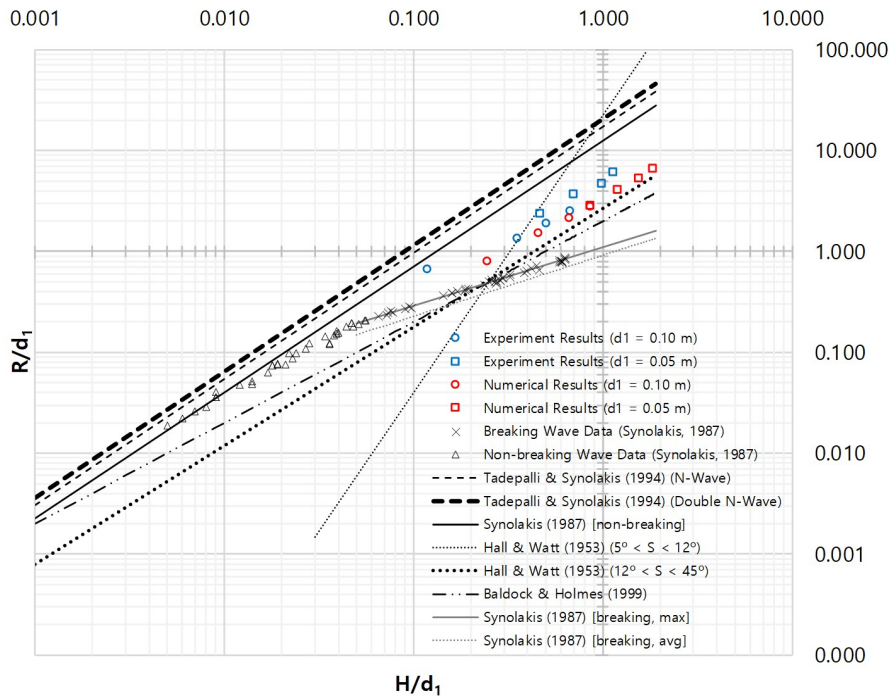


Figure 11. The relation of tsunami run-up on uniformly sloping beach and the wave height in water depth.

Figure 12 shows the maximum water level condition at different instants and at all recorded points along the slope of the beach. As can be seen in the figure that the numerical solutions are in general higher than the physical experiment for all  $d_0/d_1$ .

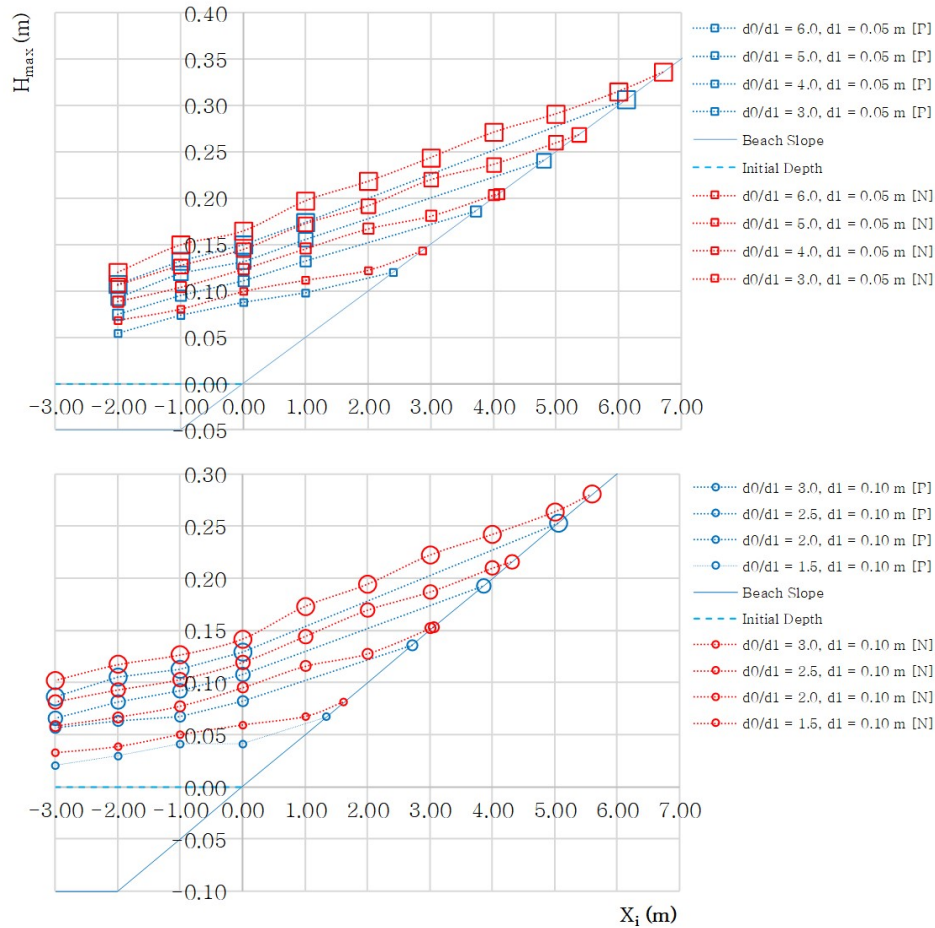


Figure 12. Comparison of physical and numerical models maximum water level along the beach slope.

The Shallow Water Equation (SWE) that assumes hydrostatic field pressure across the vertical is good enough to demonstrate tsunami motion. This is because tsunami has a larger horizontal length scale characteristic than the vertical length scale. In non-breaking waveforms conditions such as solitary and cnoidal waves, the SWE model can predict the run-up height and the run-up process in the coastal plain (Synolakis, 1991); (Liu, et al., 1991). However, when breaking wave occurs, the SWE cannot predict the run-up motion accurately as indicated in Figure 12. This suggests that the numerical solutions have not been able to accommodate the loss of energy (due to turbulence of breaking wave) during the propagation and run-ups. An additional artificial energy loss is required in the numerical scheme. As mentioned in the preceding section the typical wave resulted from Dam Break method is highly turbulence. Thus, the numerical model without artificial energy reduction based on SWE produced higher results or run-up than the physical model data. The run-ups difference was in between 9.64 and 20.61%.

A similar condition was also experienced in a study conducted by Hibberd & Peregrine (1979). They mentioned that such discrepancy was due to the effect of bottom friction which has not been properly addressed. Previously, Miller (1968) mentioned that besides coastal slope factors, bottom roughness also plays a role in determining run-up. This implied that in real cases, energy loss due to bottom roughness needs to be considered. Later, a modification to the Hibberd & Peregrine (1979) model was carried out by Packwood & Peregrine (1981) by adding the Chezy term to accommodate bottom roughness. However, the physical model by Miller (1968) was still lower than the numerical model which has not been fully explained by Packwood & Peregrine (1981).

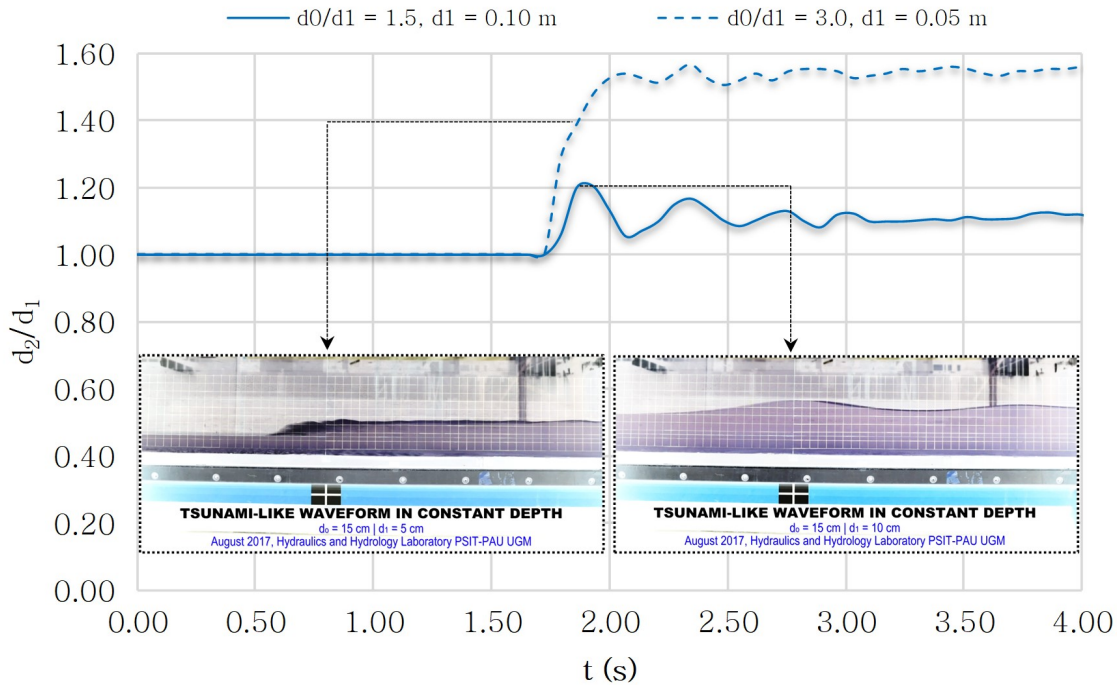


Figure 13. Typical of bore traveling in different water depth

In Figure 11, analytical and empirical solutions from some previous studies are depicted. The Run-up Law that was proposed by Synolakis (1987) is applicable for non-breaking solitary run-up. The theoretical run-up water level was above both the present physical and numerical models. This higher estimate was also experienced by Zelt (1991) when comparing the results of three models. The non-dispersive model produced higher run-up than both the dispersive model and physical experiment. In addition to Run-up Law, Synolakis (1987) also proposed the maximum and average run-up for breaking waves. These equations are also plotted in Figure 11. Synolakis (1987) solution for breaking wave was below both the present numerical and physical model results. Different type of waveforms or surge, namely solitary and bore, were most likely the reason for this deviation. This can be explained by focusing on the physical model data for  $H/d_1 = 0.118$  which yields  $R/d_1 = 0.672$  and it tends to approach the theoretical line of Run-up Law. The value of  $H/d_1 = 0.118$  is produced when  $d_0/d_1 = 1.5$  and  $d_1 = 0.10$  m. This condition produced undular bore type which did not break. These two series or wave train are shown in Figure 13. The undular bore type, however, changed to breaking wave as it approached the shore (Figure 6) and released some of its energy.



Other solutions in Figure 11 also deviate from both the present numerical and physical results. Similarly, this was probably due to different characteristics of the incoming wave such as wind wave, solitary, N-wave and Double N-Wave by Baldock & Holmes (1999), Hall & Watt (1953), and Tadepalli & Synolakis (1994), respectively.

Other solutions in Figure 11 also deviate from both the present numerical and physical results. Similarly, this was probably due to different characteristics of the incoming wave such as wind wave, solitary, N-wave and Double N-Wave by Baldo

## 1. CONCLUSION AND RECOMMENDATION

The generation of tsunami using the Dam Break method produced surge wave that breaks in shallow water and inland, similar to tsunami that approaches and finally arrives on the coast (run-up mode). The behavior of tsunami surge that propagates in water and land by using Dam Break method depends on the reservoir depth and downstream depth. At a constant depth, when  $d_0/d_1 \geq 2.0$  the surge wave produced fully developed bore and partly developed bore categories while the undular bore category was formed when  $d_0/d_1 < 2.0$ . The front celerity agree with the analytical solution of Chanson (2005). The comparison between physical and numerical models suggested that the numerical model consistently produce slightly higher run-up than its counterpart. This was probably due to the application of shallow water equation (SWE) in the numerical model that is unable to solve vertical convection problems, breaking waves, and turbulence-related aspects. Nevertheless, important characteristics in tsunami simulations such as propagation, run-up, and inundation have been successfully simulated by the addition of terms to the governing equations based on the SWE.

## ACKNOWLEDGMENT

The research was fully funded by Lembaga Pengelola Dana Pendidikan (LPDP) Kementerian Keuangan Republik Indonesia via Scholarship of Indonesia Education (BPI). We would like to express our sincere gratitude for the funding.

## REFERENCES

- Arnason, H., Petroff, C. & Yeh, H., 2009. Tsunami Bore Impingement onto a Vertical Column. *Journal of Disaster Research*, 4(6), pp. 391-403.
- Baldock, T. E. & Holmes, P., 1999. Simulation and Prediction of Swash Oscillations on a Steep Beach. *Coastal Engineering*, 36, pp. 219-242.
- Benazir, Triatmadja, R., Rahardjo, A. P. & Yuwono, N., 2016a. *Tsunami Run-up on Sloping Beach based on Dam Break System*. Bali, The 5th International Seminar of HATHI, 29-31 July 2016, pp. 565-574.

- Benazir, Triatmadja, R., Rahardjo, A. P. & Yuwono, N., 2016b. *Modeling of Tsunami Run-up onto Sloping Beach and its Interaction with Low Structure*. Yogyakarta, The 4th International Conference on Sustainable Built Environment (ICSBE), 12-14 October 2016, pp. 622-630.
- Chanson, H., 2005. *Applications of Saint-Venant Equations and Method of Characteristic to the Dam Break Wave Problem*, Brisbane, Australia: Report CH55/05, Departement of Civil Engineering The University of Queensland.
- Chanson, H., 2006. Tsunami Surges on Dry Coastal Plains: Application of Dam Break Wave Equations. *Coastal Engineering Journal*, 48(4), pp. 355-370.
- Freeman, J. C., and Le Mehaute B., 1964. Wave Breakers on a Beach and Surges on a Dry Bed, *J. Hydraulic Div. Am. Soc. Civil Engrs.*, 90, pp. 187-216.
- Goto, C., Ogawa, Y., Shuto, N. & Imamura, F., 1997. *Numerical Method of Tsunami Simulation with Leap-Frog Scheme*, IOC Manual: IUGG/IOC Time Project, UNESCO.
- Hall, J. V. & Watt, G. W., 1953. *Laboratory Investigation of The Vertical Rise of Solitary Wave on Impermeable Slopes*, Washington DC: Army Coastal Engineering Research Centre, Tech Memo 33.
- Hibberd, S. & Peregrine, D. H., 1979. Surf and Run-up on a Beach: A Uniform Bore. *Fluid Mechanics*, 95(Part 2), pp. 323-345.
- Imamura, F., Yalciner, A. C. & Ozyurt, G., 2006. *Tsunami Modelling Manual (TUNAMI Model)*. Sendai: Disaster Control Research Center, Tohoku University.
- Kaplan, K., 1955. *Generalized Laboratory Study of Tsunami Run-up*, US Army Corps of Engineers, Tech Memo, 60.
- Kuswandi, Triatmadja, R. & Istiarto, 2017. Simulation of Scouring around a Vertical Cylinder due to Tsunami. *Science of Tsunami Hazards*, 36(2), pp. 59-69.
- Li, Y. & Raichlen, F., 2003. Energy Balance Model for Breaking Solitary Wave Runup. *Journal of Waterway, Port, Coastal, Ocean Engineering*, 129, pp. 47-59.
- Liu, P. L. -F., Synolakis, C. E. & Yeh, H. H., 1991. Report on the International Workshop on Long-Wave Run-up. *J. Fluid Mech.*, 229, pp. 675-688.
- Lukkunaprasit, P., Ruangrassamee, A. & Thanasisathit, N., 2009. Tsunami Loading on Building with Opening. *Science of Tsunami Hazard*, 28(5), pp. 303-310.
- Miller, R. L., 1968. Experimental Determination of Run-up of Undular and Fully Developed Bore. *Journal of Geophysical Research*, 77(14), pp. 4497-4510.
- Packwood, A. R. & Peregrine, D. H., 1981. *Surf and Runup on beaches: Models of Viscous Effects*, England: Rep. AM-81-07, University of Bristol.
- Shen, M. C. & Meyer, R. E., 1963. Climb of a Bore on a Beach (Part 3: Run-up). *Fluid Mechanics*, 16, pp. 113-125.

- Shuto, N., 1967. Run-up of Long Waves on a Sloping Beach. *Coastal Engineering in Japan*, 10, pp. 23–38.
- Shuto, N., 1997. A Natural Warning of Tsunami Arrival. In: H. G., ed. *Perspectives on Tsunami Hazard Reduction*. Dordrecht, The Netherlands: Springer, pp. 157-173.
- Synolakis, C. E., 1986. *The Runup of Long Wave*. Ph.D Thesis ed. California: California Institute of Technology.
- Synolakis, C. E., 1987. The Runup of Solitary Waves. *Journal of Fluid Mechanics*, 185, pp. 523-545.
- Synolakis, C. E., 1991. Tsunami Runup on Steep Slopes: How Good Linear Theory Really Is. *Natural Hazards*, 4, pp. 221-234.
- Synolakis, C. E. & Bernard, E. N., 2006. Tsunami Science before and beyond Boxing Day 2004. *Philosophical Transactions of The Royal Society A*, 364, pp. 2231-2265.
- Tadepalli, S. & Synolakis, C. E., 1994. The Run-Up of N-Waves on Sloping Beaches. *Proc. R. Soc. Lond. A*, 445, pp. 99-112.
- Tadepalli, S. & Synolakis, C. E., 1996. Model for The Leading Waves of Tsunami. *Physical Review Letters*, 77(10), pp. 2141-2144.
- Triatmadja, R., 2010. *Tsunami, Kejadian, Penjalaran, Daya Rusak, dan Mitigasinya*. Yogyakarta: Gadjah Mada University Press.
- Triatmadja, R. & Benazir, 2014. Simulation of Tsunami Force on Rows of Buildings In Aceh Region After Tsunami Disaster In 2004. *Science of Tsunami Hazard*, 33(3), pp. 156-169.
- Triatmadja, R. & Nurhasanah, A., 2012. Tsunami Force on Buildings with Openings and Protection. *Journal of Earthquake and Tsunami*, 6(4), pp. 1-17.
- Togashi, H., 1981. *Study on Tsunami Run-up and Countermeasure*. Ph.D Thesis, Tohoku University.
- Yeh, H. H., 1991. Tsunami Bore Runup. *Natural Hazard*, 4, pp. 209-220.
- Yeh, H. H. & Ghazali, A., 1986. *Nearshore Behavior of Bore on a Uniformly Sloping Beach*. Taipei, Proc. 20th Cm. Coastal Engineering, pp. 877-888.
- Yeh, H. H., Ghazali, A. & Marton, I., 1989. Experimental Study of Bore Runup. *Fluid Mechanics*, 206, pp. 563-578.
- Zelt, J. A., 1991. The Run-up of Nonbreaking and Breaking Solitary Waves. *Coastal Engineering*, 15, pp. 205-246.
- Zhao, X. L., Wang, B. & Liu, H., 2012. Characteristics of Tsunami Motion and Energy Budget During Runup and Rundown Processes over a Plane Beach. *Physics of Fluids*, Volume 24.